*Journal of Ceramic Processing Research. Vol. 12, No. 5, pp. 572~577 (2011)*

J O U R N A L O F
**Ceramic Processing Research**

# Characteristics of $La_{0.8}Sr_{0.2}Ga_{(0.8x)}Mg_{0.2}O_{3-\delta}$ (x = 0.85, 0.9, 0.95, 1) electrolytes formed from powders prepared by spray pyrolysis

**Dae Soo Jung[a], Jung Hyun Kim[a], Hye Young Koo[a], You Na Ko[a], Yoon Ho Cho[b], Jong-Heun Lee[b] and Yun Chan Kang[a,*]**

[a]*Department of Chemical Engineering, Konkuk University, 1 Hwayang-dong, Gwangjin-gu, Seoul 143-701, Korea*
[b]*Department of Materials Science and Engineering, Korea University, Anam-dong, Sungbuk-ku, Seoul 136-713, Korea*

**$La_{0.8}Sr_{0.2}Ga_{(0.8x)}Mg_{0.2}O_{3-\delta}$ (LSGM) (x = 0.85, 0.9, 0.95, 1) precursor powders were prepared by spray pyrolysis from spray solutions with various Ga contents. The pellets fired at 1400 °C had dense structures without pores, irrespective of the Ga content of the powders. The grain sizes of the pellets formed from powders with low Ga contents were larger than those of the pellets formed from powders with stoichiometric Ga contents. At firing temperatures of 1300 °C and 1400 °C, phase-pure LSGM pellets were obtained from powders with a stoichiometric amount of 85 at.% Ga (x = 0.85), as was evident from the results of crystal structure analysis. An orthorhombic–rhombohedral phase transition occurred in the pellets formed from powders with stoichiometric amounts of 95 at.% (x = 0.95), and 85 at.% (x = 0.85) Ga at a firing temperature of 1400 °C. The conductivities of LSGM with orthorhombic and rhombohedral structures sintered at 1400 °C were 0.007 S/cm and 0.022 S/cm, respectively, at a low measurement temperature of 600 °C.**

**Key words: Spray pyrolysis, Solid electrolyte, Nano powder, Fuel cells.**

## Introduction

Solid oxide fuel cells (SOFCs) are gaining attention because their efficiency and fuel flexibility are better than those of other fuel cells [1, 2]. SOFCs operating at temperatures above 800 °C are termed high-temperature SOFCs. Yttria-stabilized zirconia (YSZ) is used as the electrolyte in high-temperature SOFCs [3, 4]. SOFCs operating at temperatures below 800 °C are termed intermediate-temperature or low-temperature SOFCs, depending on the operating temperature. Studies have been carried out on the feasibility of using doped lanthanum gallate oxide $La_{1-x}Sr_xGa_{1-y}Mg_yO_{3-\delta}$ (LSGM) as the electrolyte in low-temperature SOFCs; this is because of the high ionic conductivity of this compound at low temperatures [5-7]. LSGM electrolytes are expected to have good chemical homogeneity and a low porosity at low sintering temperatures.

The use of LSGM electrolytes in various solid-state reactions and liquid solution methods has been studied [5, 7, 8-11]. However, it is difficult to obtain phase-pure LSGM powders under mild preparation conditions since the product is contaminated with various intermediate phases formed, such as $LaSrGa_3O_7$, $LaSrGaO_4$, and $La_4Ga_2O_9$ [4, 12, 13]. The sintering characteristics of LSGM electrolytes are affected by the mean size, morphology, and phase homogeneity of the LSGM powders.

Spray pyrolysis, a gas-phase reaction, has been successfully used for the synthesis of multicomponent ceramic powders with good phase homogeneity [14]. Electrolyte powders with various compositions have been prepared by spray pyrolysis for use in SOFCs, and the characteristics of these powders have been studied extensively [15-17]. However, very few studies have focused on the preparation of LSGM electrolytes by spray pyrolysis.

In this study, LSGM powders were prepared by spray pyrolysis from spray solutions with various Ga contents. The Ga content of the spray solution affected the crystal structures of the prepared LSGM powders. The electrolytic characteristics of LSGM powders with various Ga contents were studied.

## Experimental procedure

The precursor powders of $La_{0.8}Sr_{0.2}Ga_{(0.8\cdot x)}Mg_{0.2}O_{3-\delta}$ (x = 0.85, 0.9, 0.95, 1) electrolytes were prepared by spray pyrolysis. A 1.7-MHz ultrasonic spray generator with six vibrators was used to generate a large number of droplets, which were carried to a high-temperature tubular reactor by a carrier gas. Droplets and powders evaporated, decomposed, and/or crystallized in the quartz reactor. The length and diameter of the quartz reactor were 1200 mm and 50 mm, respectively. The spray solution was prepared by dissolving lanthanum nitrate hexahydrate (Yakuri, 97%), strontium nitrate (Junsei, 97%), gallium nitrate hexahydrate (Aldrich, 99.99%), and magnesium nitrate hexahydrate (Junsei, 99%) in distilled water. The total concentration

*Corresponding author:
Tel : +82-2-2049-6010
Fax: +82-2-458-3504
E-mail: yckang@konkuk.ac.kr

of the La, Sr, Ga, and Mg components was fixed at 0.5 M. The flow rate of air used as the carrier gas was 20 Lminute$^{-1}$. The precursor powders obtained by spray pyrolysis at 900 ºC were post-treated in a box furnace and maintained at 1000 ºC for 6 h at a heating rate of 5 K·minute$^{-1}$. The post-treated powders were pressed into pellets using a uniaxial hydraulic press and subjected to cold isostatic pressing at 200 MPa. The pellets with diameter and thickness of 4.9 and 2.6 mm were sintered at 1300 ºC and 1400 ºC for 5 h at a heating rate of 5 K·minute$^{-1}$. Pt electrodes were fabricated on both sides of the pellets by coating the sides with Pt paste. The Pt-coated pellets were calcined at 1000 ºC for 1 h at a heating rate of 5 K·minute$^{-1}$.

The crystal structures of the calcined LSGM powders were studied by X-ray diffraction (XRD, Rigaku, D/MAX-RB) using Cu Ka radiation ($\lambda = 1.5418 \times 10^{-10}$ m). The morphological characteristics of the powders were investigated by scanning electron microscopy (SEM, JEOL, JSM 6060). The grain size and microstructure of the pellets were determined by SEM observations. The impedance of the pellets was measured with a dielectric/impedance analyzer (Model Alpha-N, Novocontrol, Germany) in range of frequency from $10^{-1}$ to $10^{7}$ Hz with an AC amplitude of 0.1 mV.

## Results and Discussion

The morphology of the precursor powders of LSGM prepared by spray pyrolysis is shown in Fig. 1. The precursor powders had a spherical shape and non-aggregated characteristics, irrespective of the Ga content of the spray solutions.

The LSGM precursor powders obtained by spray pyrolysis were post-treated at 1000 ºC for 6 h. The main peaks in the XRD patterns of the post-treated powders (Fig. 2) were attributable to LSGM, irrespective of the Ga content of the spray solutions. However, the impurity phases in the powders, such as $LaSrGa_3O_7$ and $LaSrGaO_4$, decreased with a decrease of x in $La_{0.8}Sr_{0.2}Ga_{(0.8x)}Mg_{0.2}O_{3-\delta}$. Moreover,

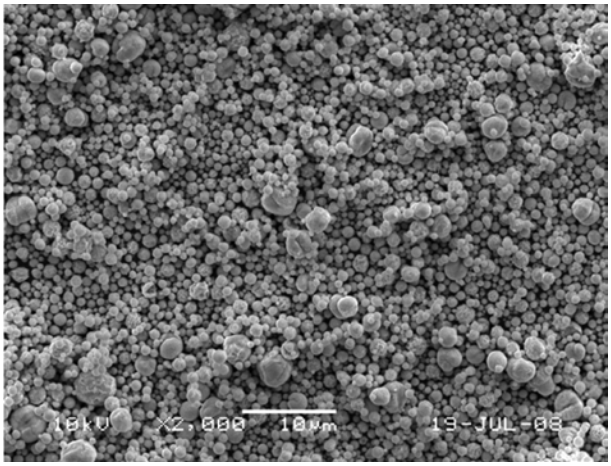


**Fig. 1.** SEM image of the precursor powder prepared by spray pyrolysis.

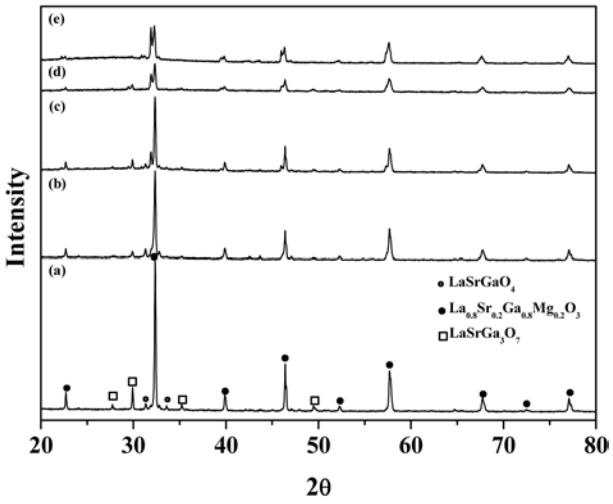


**Fig. 2.** XRD patterns of powders post-treated at 1000 ºC: (a) x = 1, (b) x = 0.95, (c) x = 0.9, (d) x = 0.85, (e) x = 0.8.

the crystal structure of LSGM was affected by the Ga content of the spray solution. $La_{0.8}Sr_{0.2}Ga_{(0.8x)}Mg_{0.2}O_{3-\delta}$ (x = 1) had a cubic crystal structure, but with a decrease in the Ga content, the crystal structure became hexagonal. This change was confirmed from the characteristic splitting of the (110) peak corresponding to the cubic phase into (110) and (104) reflections corresponding to the hexagonal phase at $2\theta \approx 32^{o}$ [18].

The SEM micrographs (Fig. 3) of the powders post-treated at 1000 ºC reveal that these powders are spherical, irrespective of the Ga content of the spray solutions. The morphologies of the precursor powders remain unchanged after the post-treatment.

The firing characteristics of the powders obtained from spray solutions with various Ga contents were investigated. The powders post-treated at 1000 ºC were pressed into pellets using a uniaxial hydraulic press and then subjected to cold isostatic pressing at 200 MPa. Figs. 4 and 5 show the SEM images of the surface of the LSGM pellets

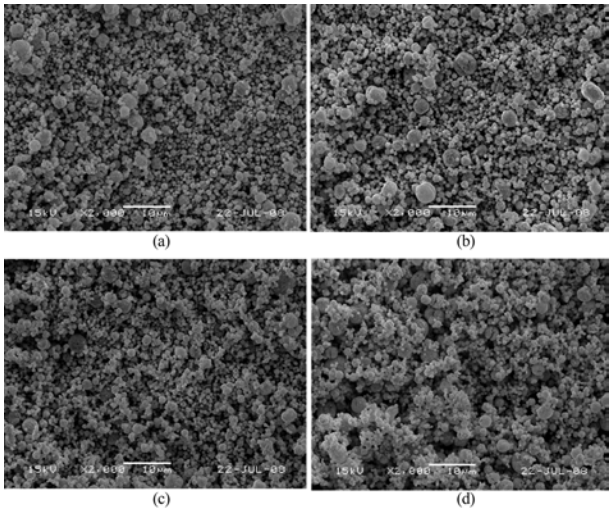


**Fig. 3.** SEM images of post-treated powders post-treated at 1000 ºC : (a) x = 1.0, (b) x = 0.95, (c) x = 0.9, (d) x = 0.85.

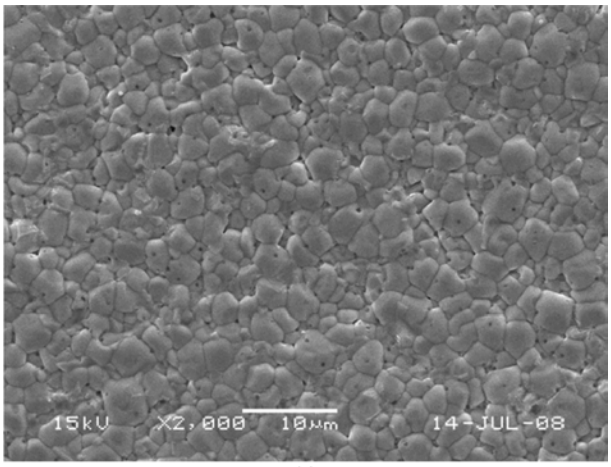


(a)

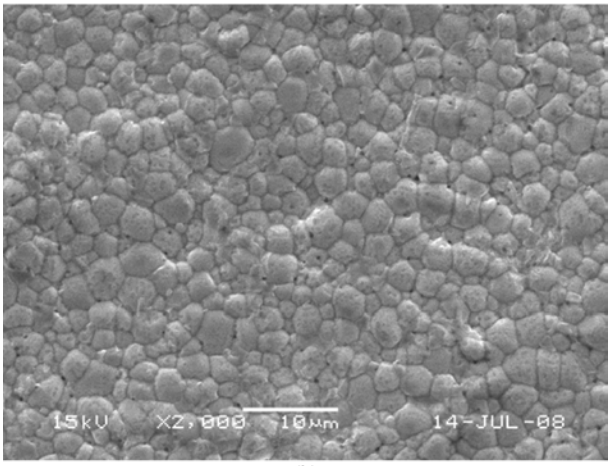


(b)

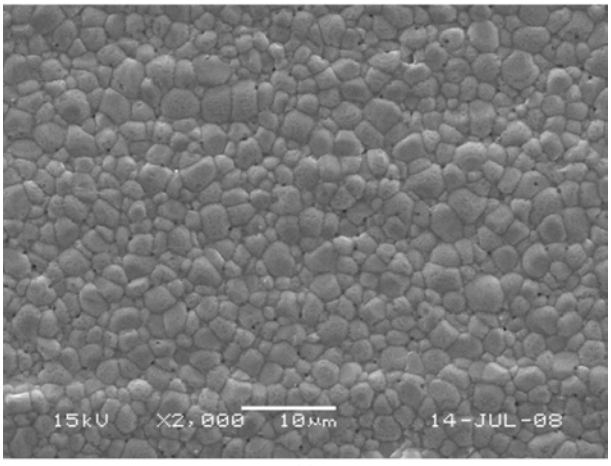


(c)

**Fig. 4.** SEM images of $La_{0.8}Sr_{0.2}Ga_{(0.8-x)}Mg_{0.2}O_{3-\delta}$ pellets sintered at 1300 ºC : (a) x = 1.0, (b) x = 0.95, (c) x = 0.85.

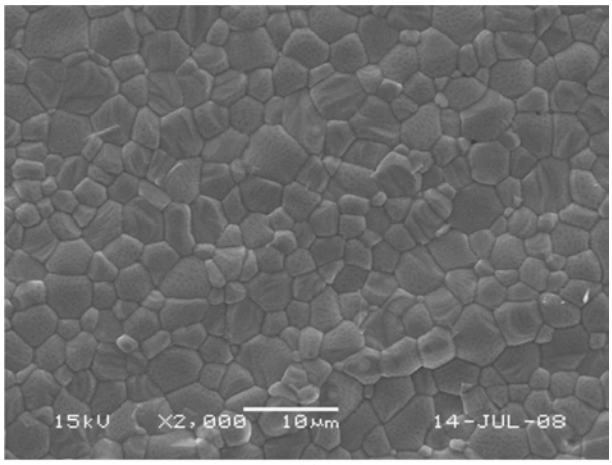


(a)

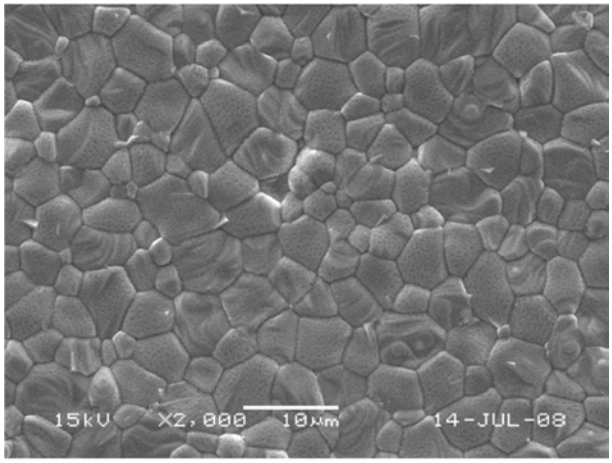


(b)

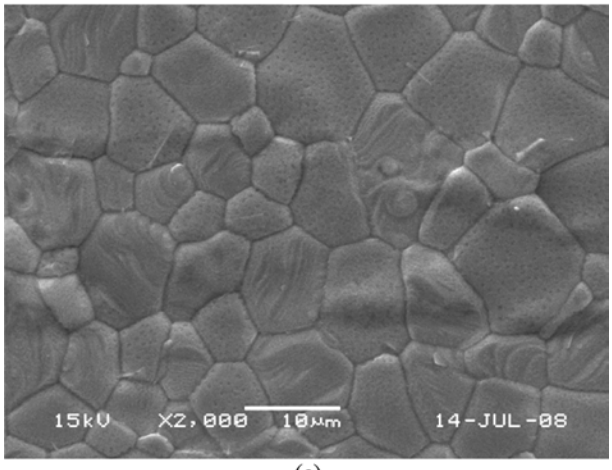


(c)

**Fig. 5.** SEM images of $La_{0.8}Sr_{0.2}Ga_{(0.8-x)}Mg_{0.2}O_{3-\delta}$ pellets sintered at 1400 ºC : (a) x = 1.0, (b) x = 0.95, (c) x = 0.85.

fired at 1300 ºC and 1400 ºC, respectively. Sintering of the pellets occurred at 1300 ºC, irrespective of the Ga content of the powders. The pellets fired at 1300 ºC had numerous small pores and similar grain sizes irrespective of the Ga content of the powders. Considerable grain growth occurred in the pellets after firing at 1400 ºC. The pellets formed from the powders with a low Ga content had a larger grain size than those formed from the powders with a stoichiometric Ga content after firing at 1400 ºC. The mean grain sizes of the pellets shown in Figs. 5(a),

5(b), and 5(c), were 3.1 μm, 3.6 μm, and 6.8 μm, respectively. The pellets fired at 1400 °C had dense structures without pores, irrespective of the Ga content of the powders.

Fig. 6 shows the XRD patterns of the LSGM pellets fired at 1300 °C and 1400 °C. The XRD patterns of the pellets formed from the powders with stoichiometric Ga contents showed small impurity peaks corresponding to the Ga-rich $LaSrGa_3O_7$ phase at 1300 °C. The peaks of the $LaSrGa_3O_7$ phase decreased with a decrease in the Ga content of the powders and an increase in the firing temperature. The results of crystal structure analysis revealed that phase-pure LSGM pellets were obtained from powders with a stoichiometric amount of 85 at.% (x = 0.85) Ga at firing temperatures of 1300 °C and 1400 °C. An orthorhombic-rhombohedral phase transition occurred at a firing temperature of 1400 °C in the pellets formed from powders with stoichiometric amounts of 95 and 85 at.% Ga contents.

Figs. 7 and 8 show the complex impedance spectra measured at 300 °C; the three low-frequency contributions in the spectra are from electrode polarization ($\rho_{ep}$), grain boundaries ($\rho^{app}_{gb}$), and grain interiors ($\rho_{gi}$). The $\rho_{gi}$ values of the LSGM pellets fired at 1300 °C and 1400 °C were similar, irrespective of the Ga content of the powders. As expected from the microstructures of the LSGM samples with different Ga contents, the $\rho^{app}_{gb}$ value decreased with an increase in the grain size. The $\rho^{app}_{gb}$ values of the LSGM pellets fired at 1300 °C were very similar, irrespective of the Ga content of the powders. In contrast, the $\rho^{app}_{gb}$ values of the LSGM pellets fired at 1400 °C decreased with the Ga content of the powders. As shown in Fig. 5, the $La_{0.8}Sr_{0.2}Ga_{(0.8x)}Mg_{0.2}O_{3-\delta}$ (x = 0.85) ceramic had the largest grain size. Thus, the smallest percentage of the grain boundary region resulted in the smallest $\rho^{app}_{gb}$ value. This difference in $\rho^{app}_{gb}$ with the grain size was in agreement with the results reported in the literature [19].

The conductivities of the pellets formed from powders

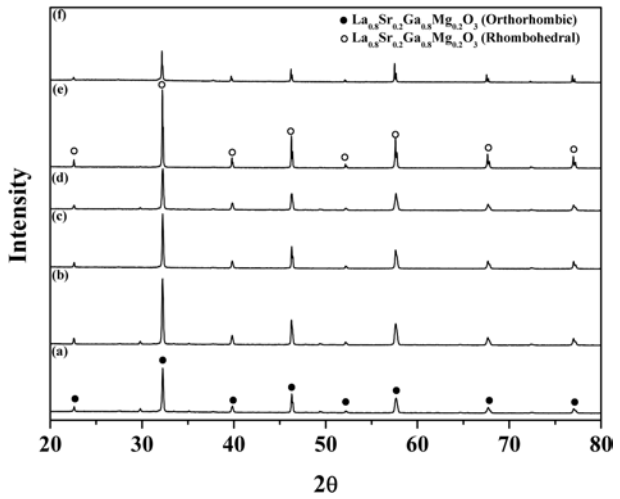


**Fig. 6.** XRD patterns of $La_{0.8}Sr_{0.2}Ga_{(0.8-x)}Mg_{0.2}O_{3-\delta}$ pellets : (a) 1300 °C, x = 1, (b) 1300 °C, x = 0.95, (c) 1300 °C, x = 0.85, (d) 1400 °C, x = 1, (e) 1400 °C, x = 0.95, (f) 1400 °C, x = 0.85.

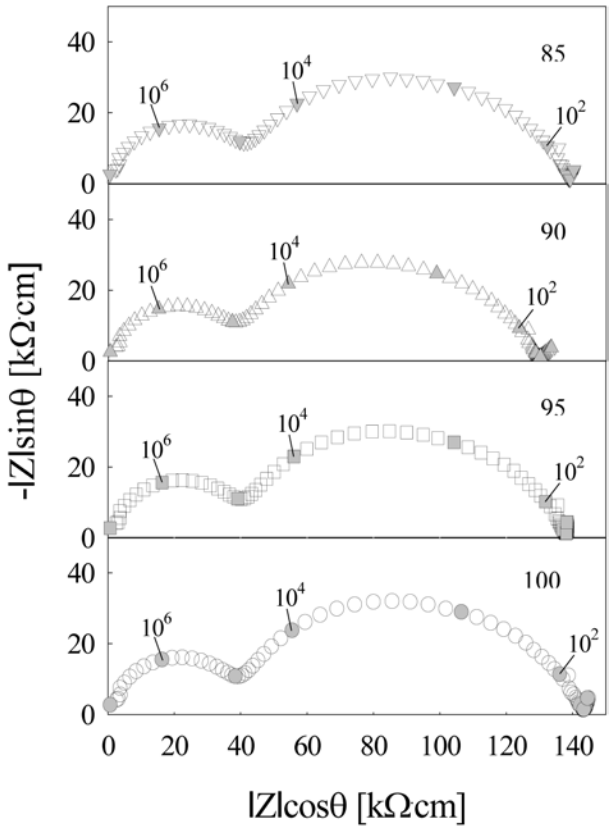


**Fig. 7.** Impedance plots of $La_{0.8}Sr_{0.2}Ga_{(0.8x)}Mg_{0.2}O_{3-\delta}$ pellets sintered at 1300 °C.

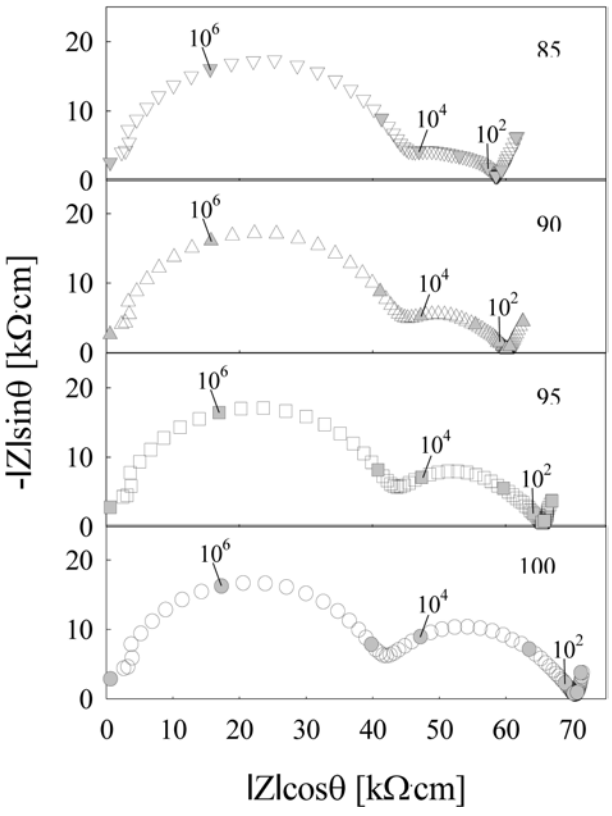


**Fig. 8.** Impedance plots of $La_{0.8}Sr_{0.2}Ga_{(0.8\times x)}Mg_{0.2}O_{3-\delta}$ pellets sintered at 1400 °C.

with various Ga contents are shown in Figs. 9 and 10. The interior resistivity ($\rho_{gi}$), the grain boundary resistivity ($\rho^{app}_{gb}$), and total resistivity ($\rho_{total}$) deconvoluted by the impedance spectrum were converted into conductivity values. As shown in Table 1, the total conductivities of the pellets fired at 1300 °C were similar at all the measurement temperatures, irrespective of the Ga content of the powders. In contrast, the conductivities of the LSGM pellets fired at 1400 °C were affected by the Ga content of the powders. The conductivity of $La_{0.8}Sr_{0.2}Ga_{(0.8x)}Mg_{0.2}O_{3-\delta}$ (x = 0.95) was considerably higher than that of $La_{0.8}Sr_{0.2}Ga_{(0.8x)}Mg_{0.2}O_{3-\delta}$ (x = 1). An orthorhombic-rhombohedral phase transition occurred in the pellets when the Ga content of the powders decreased. It has been reported that the average thermal expansion coefficient of the rhombohedral phase ($13.2 \times 10^{-6}$ $K^{-1}$) is higher than that of the cubic phase ($11.0 \times 10^{-6}$ $K^{-1}$) [20]. The thermal expansion coefficients increase with the dopant content [21]; this increase is proportional to the number of oxygen vacancies in the LSGM [21]. Therefore, the conductivity of LSGM electrolytes is affected by their crystal structure. The

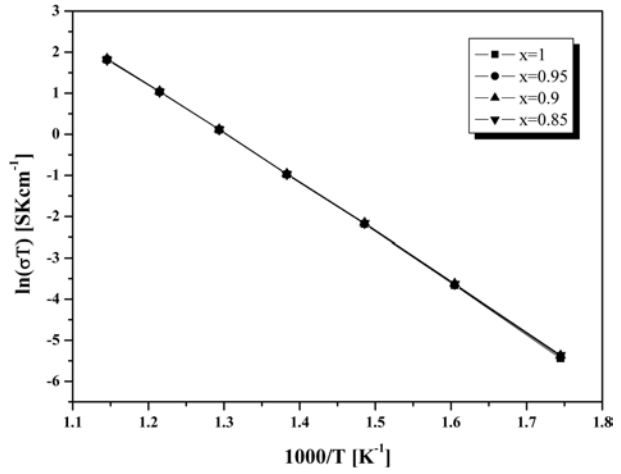


**Fig. 9.** Temperature dependence of the electrical conductivities of $La_{0.8}Sr_{0.2}Ga_{(0.8x)}Mg_{0.2}O_{3-ä}$ pellets sintered at 1300 °C.

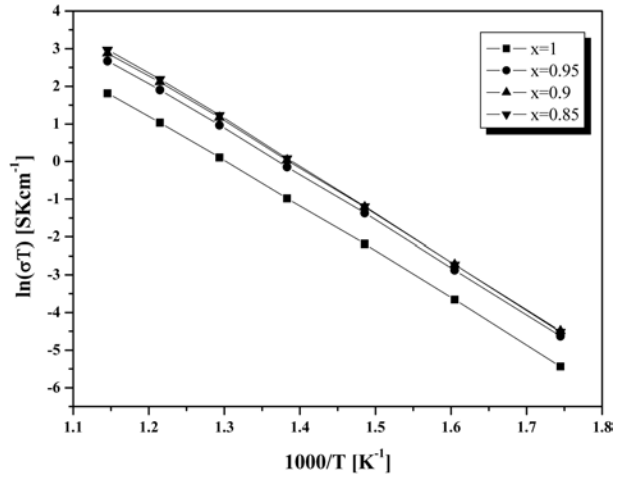


**Fig. 10.** Temperature dependence of the electrical conductivities of $La_{0.8}Sr_{0.2}Ga_{(0.8x)}Mg_{0.2}O_{3-ä}$ pellets sintered at 1400 °C.

**Table 1.** Average grain sizes, crystal structures and total conductivities of LSGM pellets sintered at 1300 and 1400 °C.

| | Grain size (μm) | Crystal structure | Conductivity at 600 °C (S/cm) |
|---|---|---|---|
| $La_{0.8}Sr_{0.8}Ga_{(0.8x)}Mg_{0.2}O_{3-\delta}$ | | Sintering Temp. 1300 °C | |
| X = 1 | 2.37 | Orthorhombic | 0.007 |
| X = 0.95 | 2.32 | Orthorhombic | 0.007 |
| X = 0.85 | 2.20 | Orthorhombic | 0.007 |
| | | Sintering Temp. 1400 °C | |
| X = 1 | 3.1 | Orthorhombic | 0.007 |
| X = 0.95 | 3.6 | Rhombogedral | 0.017 |
| X = 0.85 | 6.8 | Rhombogedral | 0.022 |

conductivities of the $La_{0.8}Sr_{0.2}Ga_{(0.8x)}Mg_{0.2}O_{3-\delta}$ (x = 0.95) and $La_{0.8}Sr_{0.2}Ga_{(0.8x)}Mg_{0.2}O_{3-\delta}$ (x = 1) electrolytes were 0.017 S/cm and 0.007 S/cm, respectively, at a low measurement temperature of 600 °C. When x was changed from 0.95 to 0.85, the conductivities of the $La_{0.8}Sr_{0.2}Ga_{(0.8x)}Mg_{0.2}O_{3-\delta}$ electrolytes with a rhombohedral structure increased from 0.017 S/cm to 0.022 S/cm at the above mentioned measurement temperature; this increase was attributed to the decreased grain boundary resistivity ($\rho^{app}_{gb}$) caused by grain growth.

## Conclusion

The effect of the Ga content of LSGM precursor powders prepared by spray pyrolysis on the characteristics of the LSGM electrolytes fired at 1300 °C and 1400 °C were investigated. The post-treated powders in which the main phase was LSGM were spherical in shape. The pellets formed from the powders with a stoichiometric amount of 85 at.% Ga content had a high phase purity, large grain size, low grain boundary resistivity, and high total conductivity.

## References

1. N.Q. Minh, Ceramic fuel cells, J. Am. Ceram. Soc. 76[3] (1993) 563-588.
2. N.Q. Minh, Solid State Ionics 174 (2004) 271-277.
3. T.H. Etsell and S.N. Flengas, Chem. Rev. 70[3] (1970) 339-376.
4. J.W. Fergus and J.W. Fergus, J. Power Sources 162 (2006) 30-40.
5. T. Ishihara, H. Matsuda and Y. Takita, J. Am. Chem. Soc. 116 (1994) 3801-3803.
6. K. Huang, R.S. Tichy and J.B. Goodenough, J. Am. Chem. Soc. 81 (1998) 2565-2575.
7. P. Huang and A. Petric, J. Electrochem. Soc. 143 (1996) 1644-1648.
8. J.W. Stevenson, T.R. Armstrong, D.E. McCready, L.R. Pederson and W.J. Weber, J. Electrochem. Soc. 144 (1997) 3613-3620.
9. A.C. Tas, P.J. Majewski and F. Aldinger, J. Am. Chem. Soc. 83 (2000) 2954-2960.

10. L.G. Cong, T.M. He and Y. Ji, J. Alloys Compd. 348 (2003) 325-331.
11. M. Shi, N. Liu, Y. Xu, Y. Yuan, P. Majewski and F. Aldinger, J. Alloys Compd. 425 (2006) 348-352.
12. Y. Zhai, C. Ye, J. Xiao and L. Dai, J. power Sources 163 (2006) 316-322.
13. N.S. Chae, K.S. Park, Y.S. Yoon, I.S. Yoo, J.S. Kim and H.H. Yoon, Colloids Surf. A: Physicochem. Eng. Aspects 313-314 (2008) 162-166.
14. A. Gurav, T. Kodas, T. Pluym and Y. Xiong, Aerosol Sci. Technol. 19 (1993) 411-452.
15. M. Gaudona, E. Djurado and N.H. Menzler, Ceram. Int. 30 (2004) 2295-2303.
16. H.S. Kang, J.R. Sohn, Y.C. Kang, K.Y. Jung and S.B. Park, J. Alloys Compd. 398 (2005) 240-244.
17. D.S. Jung, S.H. Lee, J.M. Han, H.J. Hwang, J.H. Lee and Y.C. Kang, J. Ceram. Soc. Jpn. 116 (2008) 969-974.
18. J.Y. Yi and G.M. Choi, Solid State Ionics 148 (2002) 557-565.
19. B. Rambabu, S. Ghosh, W. Zhao and H. Jena, J. Power Sources 159 (2006) 21-28.
20. W. Marti, P. Fischer, F. Altorfer, H.J. Scheel and M. Tadin, J. Phys.: Condens. Mater. 6 (1994) 127-135.
21. H. Hayashi, M. Suzuki and H. Inaba, Solid State Ionics 128 (2000) 131-139.